Cellulose (2014) 21:1611–1618
DOI 10.1007/s10570-014-0236-0

ORIGINAL PAPER

Preparation of cellulose nanocrystals and carboxylated cellulose nanocrystals from borer powder of bamboo

Yang Hu · Lirong Tang · Qilin Lu · Siqun Wang · Xuerong Chen · Biao Huang

Received: 23 December 2013 / Accepted: 9 March 2014 / Published online: 20 March 2014

Abstract Carboxylated cellulose nanocrystals (CCN) and cellulose nanocrystals (CNC) were prepared from borer powder of bamboo by two different kinds of procedures: one-step approach with ammonium persulfate for CCN and two-step approach with sulfuric acid for CNC. The obtained samples were characterizated by transmission electron microscopy, Fourier transform infrared spectroscopy, X-ray diffraction and thermogravimetric analysis. The results show that the particles of CCN and CNC present spherical shape with diameters of 20–50 and 20–70 nm, respectively. The crystallinity of CCN and CNC is significantly improved after a series of chemical treatment, which is up to 62.75 and 69.84 %, respectively. The research indicates that the borer powder from bamboo could be an excellent raw material for manufacturing CNC in a low-cost and environmental-friendly way. Rational and sustainable utilization of the bamboo borer powder to develop new bioproducts holds great potential value for industry and offers many benefits and opportunities.

Y. Hu · L. Tang · Q. Lu · X. Chen · B. Huang (✉)
College of Material Engineering, Fujian Agriculture and Forestry University, Fuzhou 350002, Fujian, China
e-mail: fjhuangbiao@hotmail.com

S. Wang
Center for Renewable Carbon, University of Tennessee, Knoxville, TN 37996-4570, USA

Keywords Bamboo borer powder · Preparation · Cellulose nanocrystals · Carboxylated cellulose nanocrystals

Introduction

Cellulose is the most abundant biomaterial on earth and has long been a major renewable source of materials (Chenampulli et al. 2012). Cellulose and its derivatives are being extensively explored for their applications in composite reinforcement, soft-tissue replacement, building materials, food packaging, etc. especially in the field of the nano-material (Li et al. 2012). Compared with natural cellulose, nanocellulose has many extraordinary advantages, such as high strength and transparency, high surface area, etc. (Tang et al. 2013). Nanocellulose has been isolated from a wide variety of sources, such as cotton, ramie, sisal, tunicate, wheat straw, wood, bamboo, etc. (Peng et al. 2011; Brito et al. 2012). The extraction processes of nanocellulose can be performed by different kinds of procedures. Many preparation methods for producing nanocellulose have previously been reported. Each method possesses its own advantages and drawbacks related to the amount/quality of cellulose (Abraham et al. 2011). Acid hydrolysis and mechanical processes have been used to extract nanocellulose from a variety of cellulose sources. Sulfuric acid (H_2SO_4) is most typically used as it produces stable colloidal

dispersion due to the grafting of sulfate ester groups on the surface of the nanocellulose, but other acids (hydrochloric acid, maleic acid) have also been used. As to the mechanical process, it generally involves high-pressure homogenizers, grinders/refiners, high intensity ultrasonic treatments and microfluidization (Moon et al. 2011).

On one hand, bamboo is one of the fastest-growing plants on Earth, with reported growth rates of 100 cm (39 in.) in 24 h (Farrelly 1996). It is estimated 20 million tons of annual production worldwide (Amada et al. 1996; Choy et al. 2005). On the other hand, bamboo is very susceptible to *lyctus brunneus*, a species of powder-post beetles, which reduces the woody material to a fine, flour-like powder within a few weeks. An enormous quantity of bamboo raw material is lost every year due to the damage from insect borers (Santhoshkumar 2005). Bamboo borer powder mainly consists of cellulose, lignin, hemicellulose and other alcohol benzene extractive like tannin, fatty acid, etc. (Sun et al. 2009). In contrast to other lignocellulosic biomasses, the borer powder has distinct advantages, i.e. the borer powder is fine flour-like powder with size of about a few dozen micrometers, which can directly be used, saving much energy and labor. In addition, the powder-post beetles are quite easy to be artificially reared in the warm area, such as Southern China. Rational and sustainable utilization of the borer powder to develop new bioproducts would be of great benefit as it not only diminishes adverse environmental impact but also creates new value-added avenue.

The study aimed mainly to explore the feasibility of using borer powder as a new potential lignocellulosic precursor for producing nanocellulose in an attempt to convert this waste into value-added products. In order to obtain nanocellulose with different performance, two methods were adopted: one-step oxidative degradation procedure with ammonium persulfate for carboxylated cellulose nanocrystals (CCN) and sulphuric acid hydrolysis of cellulose extracted from borer powder for cellulose nanocrystals (CNC) (Leung et al. 2011; Bondeson et al. 2006). In this work, the characteristics of the CCN and CNC obtained by the above two methods were investigated and their properties were analyzed so as to explore the effect of different extraction processes on the properties of the nanocellulose from borer powder by identical characterization tools and equipment.

Cellulose, hemicelluloses and lignin contents of borer powder were determined by chemical analysis as well as the uninfected bamboo powder. The morphology of borer powder and nanocellulose were investigated by scanning and transmission electron microscopy (SEM and TEM). Fourier transform infrared spectrometry (FTIR), X-ray diffraction (XRD) and thermogravimetric analysis (TGA) experiments were performed to characterize the raw material and nanocellulose.

Materials and methods

Materials

Borer powder from Mao bamboo (Fujian, China) attacked by *lyctus brunneus* was used in the study. The *lyctus brunneus* were reared naturally in environments with high relative humidity and room temperature for a few days until a large number of holes appeared on the surface of bamboo slats (2 cm × 40 cm) and powdery dust fell out of holes. The powder was collected and separated from other solids by passing through a 200-mesh screen to remove the borers' eggs and the residual piece of bamboo. The chemical compositions of borer powder and bamboo powder were determined according to TAPPI Method T 264 om-88 and a previous study (Khalil et al. 2007). Sulfuric acid (H_2SO_4), ammonium persulfate [$(NH_4)_2S_2O_8$, APS], benzene, sodium chlorite ($NaClO_2$), acetic acid (CH_3COOH), potassium hydroxide (KOH) and ethanol (CH_3CH_2OH) were purchased from Sinopharm Chemical Reagent Beijing Co. Ltd. (Beijing, China). All chemicals were of analytical reagent grade and used without any further purification.

Manufacture of cellulose nanocrystals from borer powder

Direct oxidative degradation with ammonium persulfate (one-step procedure)

The borer powder (6 g) was added to 200 mL of 2 M ammonium persulfate solution. The mixture was performed in an ultrasonic reactor KQ-250DB (Kun Shan Ultrasonic Instruments Co. Ltd., China) at 40 kHz, 65 °C for 6 h under continuous stirring at 250 r/min with a poly (tetrafluoroethylene) (PTFE)-coated stirring device. The reacted suspension was washed three times with distilled water by centrifugation (9,000 rpm,

6 min) to remove the inorganic ion until the solution pH was neutral. The CCN were collected after five times' repetitive centrifugations at 6,000 rpm for 6 min. The resulting suspension was lyophilized to yield white powder.

Cellulose extraction and sulfuric acid hydrolysis (two-step procedure)

The non-cellulosic components in borer powder were removed to obtain purified cellulose by the procedure as follows (Chen et al. 2011). Dewaxed treatment of the samples (5 g) was carried out in the Soxhlet extractor by using a 2:1(v/v) mixture of benzene/ethanol for 7 h. Afterwards, to remove lignin in the samples, bleaching was performed by using an acidified $NaClO_2$, with pH adjusted to 3.0–4.0 by CH_3COOH, at 75 °C for an hour, and the process was repeated six times, resulting in holocellulose. Then, the holocellulose was treated with 2 wt% KOH at 90 °C for 2 h to remove hemicelluloses, residual pectin and starch. The samples were washed with distilled water after each treatment. Purified cellulose powder was obtained by lyophilizing in a vacuum freeze drier.

To prepare the CNC, the extracted cellulose from borer powder was hydrolyzed with 64 wt% H_2SO_4 solution at 45 °C for 45 min under ultrasonic treatment at 40 kHz. The reaction was stopped by diluting with tenfold ice distilled water. The resulting suspension was washed with 60 % ethanol in centrifugation (9,000 rpm, 6 min) until the pH was neutral. The CNC suspension was accumulated in centrifugation (6,000 rpm, 6 min) for five times. Freeze-drying of the CNC suspension at −40 °C for 48 h resulted in powdery CNC.

Characterization

The surface morphologies and microstructures of borer powder and the extracted cellulose were analyzed on a XL30 ESEM-TMP ESEM (Philips-FEI, Netherlands) with an accelerating voltage of 1 kV and energy resolution of 129 eV. All the samples were sputtered and coated with gold.

H7650 TEM (Hitachi, Ltd., Japan) with acceleration voltage of 200 kV was used to observe the morphology and size of the CCN and CNC. The nanocellulose suspension was stained with a 2 wt% solution of phosphotungstic acid for 2 min and dried at room temperature.

FTIR was performed by means of a Nicolet 380 FTIR spectrometer (Thermo Electron Instruments Co. Ltd., USA) in the range from 400 to 4,000 cm^{-1} at a 4 cm^{-1} resolution. KBr pellets were prepared by mixing 1 mg of each sample with 150 mg of KBr.

XRD studies of each sample were performed by an X'Pert Pro MPD X-ray diffractometer (Philips-FEI, Netherlands) with Cu Kα radiation at a wavelength $\lambda = 0.154$ nm in the range $2\theta = 6°–90°$ at a speed of 0.1°/min. The empirical Eq. (1) in the study of (Segal et al. 1959) was used to calculate the crystallinity index (CrI).

$$\mathrm{CrI} = \frac{(I_{200} - I_{am})}{I_{200}} \times 100 \quad (1)$$

where I_{200} is the diffracted intensity of the crystalline segments at the peak about $2\theta = 22°$ and I_{am} is the diffracted intensity of the amorphous regions at about $2\theta = 18°$.

The thermal stability of each sample was determined by a thermogravimetric analyzer (NETZSCH STA 449F3, Germany) under N_2 atmosphere. The temperature range from 25 to 600 °C was maintained at the heating rate of 10 °C/min.

Results and discussion

Chemical composition

The chemical composition of borer powder and the uninfected bamboo powder is shown in Table 1. The uninfected bamboo powder consists of 37.5 % cellulose, 27.8 % hemicellulose, 27.9 % lignin, and 4.5 % organic solvent extracts, while the corresponding content of borer powder is 35.7, 30.4, 27.3, and 4.6 %, respectively. This shows that there is little difference in the chemical composition between the uninfected bamboo powder and borer powder due to the fact that borer powder is just the residuum of bamboo produced by powder-post beetles after the cell content of bamboo is attacked, such as starch, sugars, etc.

Morphological analysis

Figure 1 shows the macroscopic images of the bamboo sheets attacked by powder-post beetles, powder-

Table 1 Chemical composition of the uninfected bamboo powder and borer powder

Samples	α-Cellulose (%)	Lignin (%)	Holocellulose (%)	Extractive (%)	Ash (%)
Bamboo powder	37.5 ± 1.4	27.8 ± 0.6	65.4 ± 0.9	4.5 ± 0.3	1.2 ± 0.2
Borer powder	35.7 ± 1.8	27.3 ± 0.7	66.1 ± 1.3	4.6 ± 0.6	0.9 ± 0.4

Fig. 1 Photographs of *a* the infected bamboo sheets, *b* powder-post beetles, *c* borer powder, and *d* CCN and CNC suspension

post beetles, borer powder and the suspension of CCN and CNC. The powder was obtained from the frass by passing through a 200-mesh screen to remove the eggs and the residual piece of bamboo. The color of the powder is light yellowish and the particle is fine and even. The CCN and CNC suspensions have a white gel appearance and display a colloidal nature. The concentrations are 0.5 and 0.7 %, respectively.

The ESEM images clearly show the micro-morphology of borer powder (Fig. 2a) and the extracted cellulose (Fig. 2b). The particles of the powder were irregularly-shaped chewed fragments. The surface of fragments appeared uneven and torn, with the size being 10–50 μm. On the contrary, after a series of chemical treatment, the cellulose isolated from borer powder was even flake with smooth surface, similar to fish scale with thickness around 0.5 μm and diameter around 30 μm.

TEM observation of CCN and CNC shows nano-scale spheres or nanoparticles (Fig. 2c, d). Some subtle differences in morphologies and dimensions were also observed between them. The CCN particles had a spherical shape with the diameters range from 20 to 50 nm. In contrast, CNC particles were roughly

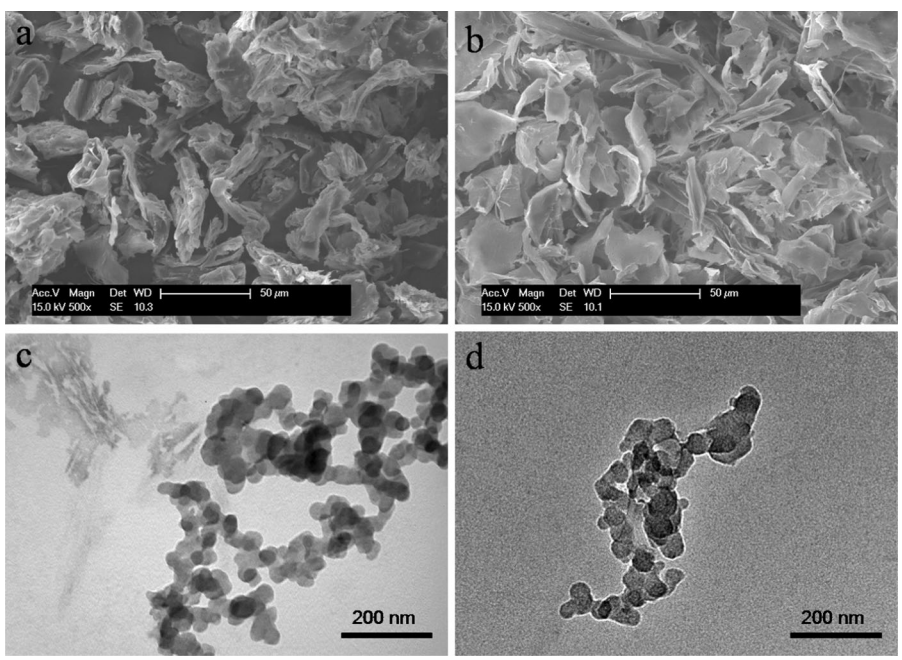

Fig. 2 ESEM of **a** borer powder and **b** the extracted cellulose, TEM of **c** CCN and **d** CNC

spherical and had the diameter range of 20–70 nm, with majority between 30 and 50 nm. It seemed that the aggregations of CCN and CNC did occur to form larger particles due to interfacial hydrogen bonds. The aggregative trend of the CNC was more obvious, which could be ascribed to the lower negative charge on the surface of CNC than that of CCN. While spherical cellulose nanoparticles obtained from various biomass have been reported previously (Li et al. 2012; Lu and Hsieh 2010; Filson and Dawson-Andoh 2009), it is widely believed that the spherical cellulose nanoparticles were possibly created by a self-assembly process from nanocrystalline cellulose and their fragments (Lu and Hsieh 2012).

FTIR spectroscopy analysis

The FTIR spectra of borer powder, the cellulose extracted from borer powder, CCN, and CNC are illustrated in Fig. 3. The similar peaks in the four samples represent chemical structures as follows. The broad bands near to 3,400 cm^{-1} are O–H stretching vibrations and the peaks at 2,900 cm^{-1} are assigned to C–H stretching vibrations. The absorption at 1,640 cm^{-1} is related to the adsorbed water due to the presence of abundant hydrophilic hydroxide radical in the cellulose (Alemdar and Sain 2008). A peak at 1,382 cm^{-1} corresponds to C–H asymmetric deformations (Sun et al. 2005). The sharp absorption peaks at around 1,058 cm^{-1} are due to C–O stretching vibrations (Xiao et al. 2001). These spectra confirm that the chemical structure of the extracted cellulose remains the same. Compared with the borer powder, the most distinct spectral change, except CCN (Fig. 3c), is the absence of four peaks at 1,734 cm^{-1} (carbonyl stretching vibrations) (Fig. 3b, d), 1,604, 1,512, and 1,462 cm^{-1} (benzene skeleton vibration) (Fig. 3a). The carbonyl peak at 1,734 cm^{-1} shows the existence of polysaccharides, such as hemicellulose, phenolic acids, pectin and xylan. The three peaks at 1,604, 1,512, and 1,462 cm^{-1} arise from the benzene skeleton construction which is typical of the lignin. The disappearance of these peaks from the spectrum of the treated cellulose indicates the complete removal of non-cellulose materials in borer powder. On the other hand, the CCN absorption patterns maintain the peak at 1,734 cm^{-1} due to the presence of carboxylic acid groups.

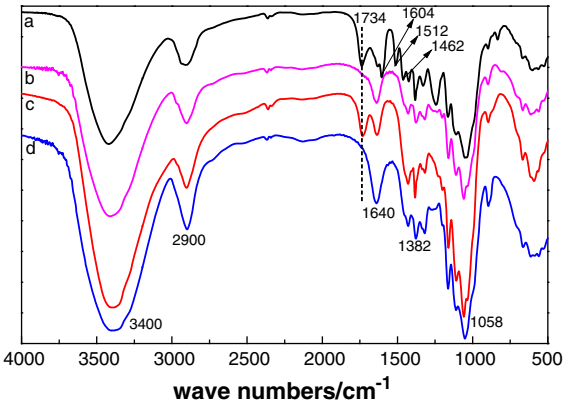

Fig. 3 FTIR spectra of *a* borer powder, *b* CNC, *c* CCN, and *d* the extracted cellulose

X-ray diffraction measurements

XRD patterns of borer powder, the extracted cellulose, CCN and CNC are shown in Fig. 4 and the corresponding crystallinity values are summarized in Table 2. Similar diffraction patterns with four diffraction peaks at 2θ value of around 15.1°, 16.5°, 22.8° and 34.6°, characteristic of cellulose crystal assignments of the $1\bar{1}0$, 110, 200 and 004 planes, respectively, were believed to represent the typical crystalline structure of cellulose I for all samples (Wada et al. 2004). The crystallinity indexes of borer powder, the extracted cellulose, CCN and CNC were calculated to be 35.94, 56.00, 62.75, and 69.84 %, respectively. The apparent change of crystallinity occurred among them. The crystallinity of the extracted cellulose increased to 56.00 % from 35.94 % of borer powder due to the removal of amorphous hemicelluloses and lignin during chemical treatment. The crystallinity indexes of CCN (62.75 %) and CNC (69.84 %) were higher than the value of 56 % for the extracted cellulose. This was ascribed to the progressive removal of the cellulose in the amorphous regions. In addition, the value of CCN was lower than that of CNC because of partial damage of crystalline structure of cellulose during the course of treatment with APS. Therefore, two kinds of high crystalline CNC were obtained by two different methods from borer powder. The high crystalline CNC could be more effective in improving the mechanical properties of the composite material, since higher crystallinity is associated with higher

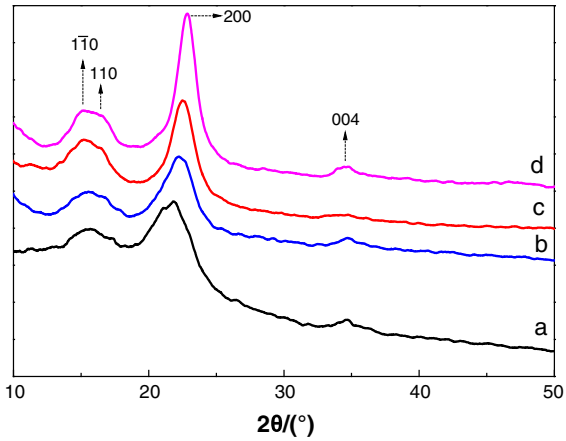

Fig. 4 XRD of *a* borer powder, *b* the extracted cellulose, *c* CCN, and *d* CNC

Table 2 Crystallinity index of borer powder, the extracted cellulose, CCN and CNC

Samples	2θ(am) (°)	2θ(200) (°)	Crystallinity index (%)
Borer powder	18.126	22.006	35.94
The extracted cellulose	18.195	22.055	56.00
CCN	18.766	22.446	62.75
CNC	18.575	22.575	69.84

tensile strength of the material (Bhatnagar and Sain 2005).

Thermogravimetric analysis

TGA and differential thermogravimetric (DTG) curves of borer powder, the extracted cellulose, CCN and CNC are shown in Fig. 5a, b, respectively. The corresponding data, including the onset temperature, the temperature of maximum weight-loss rate (T_{max}), and weight loss (WL) are listed in Table 3. The results showed that the slight WL below 100 °C was caused by evaporation of imbibed water from the samples. The onset decomposition temperature of the extracted cellulose and CCN, 297.8 and 283.8 °C, respectively, was higher than that at 274.5 °C for borer powder. This lower degradation temperature for the raw powder could be due to the hemicelluloses component. Hemicelluloses were embedded within and between the cellulose fibrils (Sheltami et al. 2012). On one hand, the hemicelluloses decomposed before lignin

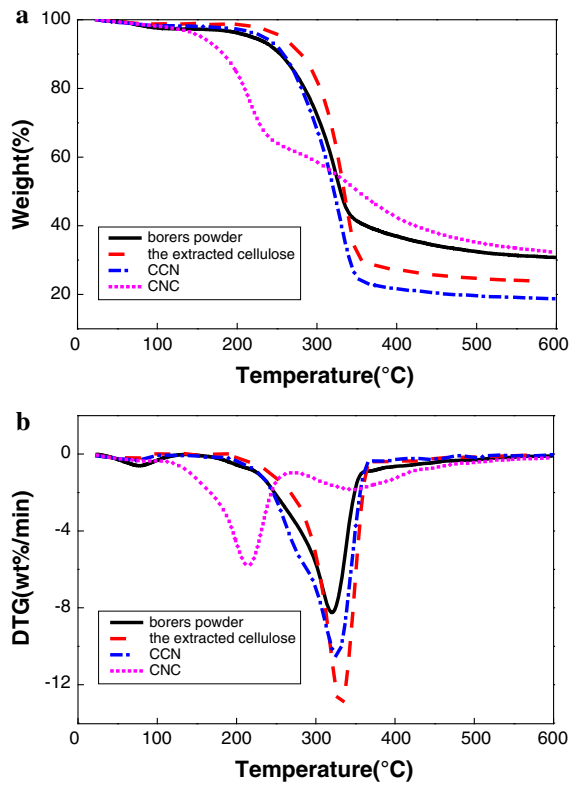

Fig. 5 **a** TG and **b** DTG curves for borer powder, the extracted cellulose, CCN and CNC

and cellulose due to the presence of acetyl groups in the hemicelluloses molecules (Shebani et al. 2008). On the other hand, the strong combination between cellulose and hemicelluloses was believed to decrease the crystallinity of cellulose and accelerate the beginning of the thermal degradation process (Sheltami et al. 2012; Deepa et al. 2011). Additionally, the CNC exhibited the lowest thermal stability at the decomposition temperature of 180.1 °C and obvious differences in the degradation behaviors. As for the CNC obtained from sulfuric acid hydrolysis, the degradation occurred within a wider temperature range and showed two well-separated pyrolysis processes. The first process in CNC had about 36.43 % WL, while the WL in the second process decreased to 22.01 %. For the first process, the high surface area of CNC might play an important role in diminishing their thermostability due to the increased exposure surface area to heat. Moreover, the decomposition of CNC occurring at lower temperatures from 107 to 276 °C might also indicate faster heat transfer in CNC. The CNC have been reported to function as efficient pathways for

Table 3 Onset temperature, degradation temperature, T_{max} and weight loss, WL in the thermal degradation processes of the four samples obtained from the TG and DTG curves

Sample	Onset temp (°C)	T_{max} (°C)	WL (%)
Borer powder	274.5	323.9	66.5
The extracted cellulose	297.9	335.2	75.1
CCN	283.8	328.1	79.4
CNC	180.1	215.1	66.7

phonons, leading to their higher thermal conductivity (Shimazaki et al. 2007). The better thermal conductivity of CNC might be ascribed to smaller phonon scattering in the bundle of crystallized cellulose chains in the CNC than the amorphous random chains in cellulose powder (Lu and Hsieh 2010). As for the second process, the consecutive degradation reaction occurred in the cellulose crystal interior at 276–433 °C, the higher temperature process could be related to the slow charring process of the solid residue.

Conclusions

The borer powder from bamboo could be an excellent raw material for manufacturing CNC in a low-cost and environmental-friendly way. The results show that the chemical composition between the uninfected bamboo powder and borer powder hasn't been changed significantly. And the particles of CCN and CNC present spherical shape with diameters of 20–50 and 20–70 nm, respectively. The crystallinity of CCN and CNC are significantly improved after a series of chemical treatment, which is up to 62.75 and 69.84 %, respectively.

Acknowledgments We appreciate the generous financial support of the National Natural Science Foundation of China (Grant Nos. 31170520, 31370560), and Science and Technology Project of Fujian Province (2013H0004).

References

Abraham E, Deepa B, Pothan L, Jacob M, Thomas S, Cvelbar U, Anandjiwala R (2011) Extraction of nanocellulose fibrils from lignocellulosic fibres: a novel approach. Carbohydr Polym 86(4):1468–1475. doi:10.1016/j.carbpol.2011.06.034

Alemdar A, Sain M (2008) Isolation and characterization of nanofibers from agricultural residues: wheat straw and soy hulls. Bioresour Technol 99(6):1664–1671. doi:10.1016/j.biortech.2007.04.029

Amada S, Munekata T, Nagase Y, Ichikawa Y, Kirigai A, Zhifei Y (1996) The mechanical structures of bamboos in viewpoint of functionally gradient and composite materials. J Compos Mater 30(7):800–819. doi:10.1177/002199839603000703

Bhatnagar A, Sain M (2005) Processing of cellulose nanofiber-reinforced composites. J Reinf Plast Compos 24(12):1259–1268. doi:10.1177/0731684405049864

Bondeson D, Mathew A, Oksman K (2006) Optimization of the isolation of nanocrystals from microcrystalline cellulose by acid hydrolysis. Cellulose 13(2):171–180. doi:10.1007/s10570-006-9061-4

Brito BSL, Pereira FV, Putaux JL, Jean B (2012) Preparation, morphology and structure of cellulose nanocrystals from bamboo fibers. Cellulose 19(5):1527–1536. doi:10.1007/s10570-012-9738-9

Chen W, Yu H, Liu Y (2011) Preparation of millimeter-long cellulose I nanofibers with diameters of 30–80 nm from bamboo fibers. Carbohydr Polym 86(2):453–461. doi:10.1016/j.carbpol.2011.04.061

Chenampulli S, Unnikrishnan G, Sujith A, Thomas S, Francis T (2012) Cellulose nano-particles from Pandanus: viscometric and crystallographic studies. Cellulose 20(1):429–438. doi:10.1007/s10570-012-9831-0

Choy KKH, Barford JP, McKay G (2005) Production of activated carbon from bamboo scaffolding waste—process design, evaluation and sensitivity analysis. Chem Eng J 109(1–3):147–165. doi:10.1016/j.cej.2005.02.030

Deepa B, Abraham E, Cherian BM, Bismarck A, Blaker JJ, Pothan LA, Leao AL, de Souza SF, Kottaisamy M (2011) Structure, morphology and thermal characteristics of banana nano fibers obtained by steam explosion. Bioresour Technol 102(2):1988–1997. doi:10.1016/j.biortech.2010.09.030

Farrelly D (1996) The book of bamboo: a comprehensive guide to this remarkable plant, its uses, and its history. Thames and Hudson Ltd, London

Filson PB, Dawson-Andoh BE (2009) Sono-chemical preparation of cellulose nanocrystals from lignocellulose derived materials. Bioresour Technol 100(7):2259–2264. doi:10.1016/j.biortech.2008.09.062

Khalil HSA, Alwani MS, Omar AKM (2007) Chemical composition, anatomy, lignin distribution, and cell wall structure of Malaysian plant waste fibers. BioResources 1(2):220–232

Kim DY, Nishiyama Y, Wada M, Kuga S (2001) High-yield carbonization of cellulose by sulfuric acid impregnation. Cellulose 8(1):29–33. doi:10.1023/A:1016621103245

Leung AC, Hrapovic S, Lam E, Liu Y, Male KB, Mahmoud KA, Luong JH (2011) Characteristics and properties of carboxylated cellulose nanocrystals prepared from a novel one-step procedure. Small 7(3):302–305. doi:10.1002/smll.201001715

Li J, Wei X, Wang Q, Chen J, Chang G, Kong L, Su J, Liu Y (2012) Homogeneous isolation of nanocellulose from sugarcane bagasse by high pressure homogenization. Carbohydr Polym 90(4):1609–1613. doi:10.1016/j.carbpol.2012.07.038

Lu P, Hsieh YL (2010) Preparation and properties of cellulose nanocrystals: rods, spheres, and network. Carbohydr Polym 82(2):329–336. doi:10.1016/j.carbpol.2010.04.073

Lu P, Hsieh YL (2012) Cellulose isolation and core–shell nanostructures of cellulose nanocrystals from chardonnay grape skins. Carbohydr Polym 87(4):2546–2553. doi:10.1016/j.carbpol.2011.11.023

Moon RJ, Martini A, Nairn J, Simonsen J, Youngblood J (2011) Cellulose nanomaterials review: structure, properties and nanocomposites. Chem Soc Rev 40(7):3941–3994. doi:10.1039/C0CS00108B

Peng BL, Dhar N, Liu HL, Tam KC (2011) Chemistry and applications of nanocrystalline cellulose and its derivatives: a nanotechnology perspective. Can J Chem Eng 89(5):1191–1206. doi:10.1002/cjce.20554

Santhoshkumar R (2005) Distribution of starch in the culms of *Bambusa bambos* (L.) Voss and its influence on borer damage. J Am Bamboo Soc 19(1):1–4

Segal L, Creely J, Martin A, Conrad C (1959) An empirical method for estimating the degree of crystallinity of native cellulose using the X-ray diffractometer. Text Res J 29(10):786–794. doi:10.1177/004051755902901003

Shebani A, Van Reenen A, Meincken M (2008) The effect of wood extractives on the thermal stability of different wood species. Thermochim Acta 471(1):43–50. doi:10.1016/j.tca.2008.02.020

Sheltami RM, Abdullah I, Ahmad I, Dufresne A, Kargarzadeh H (2012) Extraction of cellulose nanocrystals from mengkuang leaves (*Pandanus tectorius*). Carbohydr Polym 88(2):772–779. doi:10.1016/j.carbpol.2012.01.062

Shimazaki Y, Miyazaki Y, Takezawa Y, Nogi M, Abe K, Ifuku S, Yano H (2007) Excellent thermal conductivity of transparent cellulose nanofiber/epoxy resin nanocomposites. Biomacromolecules 8(9):2976–2978. doi:10.1021/bm7004998

Sun X, Xu F, Sun R, Fowler P, Baird M (2005) Characteristics of degraded cellulose obtained from steam-exploded wheat straw. Carbohydr Res 340(1):97–106. doi:10.1016/j.carres.2004.10.022

Sun S, Guan H, Bai Y (2009) SEM observation and principal components analysis of borers powder form *Dendrocalamus hamiltonii* Nees et Arn. Ex Munro. J Cellul Sci Technol 17(3):19–22, 27. doi:10.3969/j.issn.1004-8405.2009.03.004

Tang L, Huang B, Lu Q, Wang S, Ou W, Lin W, Chen X (2013) Ultrasonication-assisted manufacture of cellulose nanocrystals esterified with acetic acid. Bioresour Technol 127:100–105. doi:10.1016/j.biortech.2012.09.133

Wada M, Heux L, Sugiyama J (2004) Polymorphism of cellulose I family: reinvestigation of cellulose IVI. Biomacromolecules 5(4):1385–1391. doi:10.1021/bm0345357

Wang N, Ding E, Cheng R (2007) Thermal degradation behaviors of spherical cellulose nanocrystals with sulfate groups. Polymer 48(12):3486–3493. doi:10.1016/j.polymer.2007.03.062

Xiao B, Sun X, Sun R (2001) Chemical, structural, and thermal characterizations of alkali-soluble lignins and hemicelluloses, and cellulose from maize stems, rye straw, and rice straw. Polym Degrad Stab 74(2):307–319. doi:10.1016/S0141-3910(01)00163-X